Molecular Neurobiology (2019) 56:892–906
https://doi.org/10.1007/s12035-018-1128-3

Wnt Signaling Pathways Are Dysregulated in Rat Female Cerebellum Following Early Methyl Donor Deficiency

Jérèmy Willekens[1] · Sébastien Hergalant[1] · Grégory Pourié[1] · Fabian Marin[1] · Jean-Marc Alberto[1] · Lucie Georges[1] · Justine Paoli[1] · Christophe Nemos[1,2] · Jean-Luc Daval[1] · Jean-Louis Guéant[1] · Brigitte Leininger-Muller[1] · Natacha Dreumont[1]

Received: 30 January 2018 / Accepted: 14 May 2018 / Published online: 26 May 2018

Abstract

Gestational methyl donor (especially B9 and B12 vitamins) deficiency is involved in birth defects and brain development retardation. The underlying molecular mechanisms that are dysregulated still remain poorly understood, in particular in the cerebellum. As evidenced from previous data, females are more affected than males. In this study, we therefore took advantage of a validated rat nutritional model and performed a microarray analysis on female progeny cerebellum, in order to identify which genes and molecular pathways were disrupted in response to methyl donor deficiency. We found that cerebellum development is altered in female pups, with a decrease of the granular cell layer thickness at postnatal day 21. Furthermore, we investigated the involvement of the Wnt signaling pathway, a major molecular pathway involved in neuronal development and later on in synaptic assembly and neurotransmission processes. We found that Wnt canonical pathway was disrupted following early methyl donor deficiency and that neuronal targets were selectively enriched in the downregulated genes. These results could explain the structural brain defects previously observed and highlighted new genes and a new molecular pathway affected by nutritional methyl donor deprivation.

Keywords Methyl donor deficiency · Cerebellum · Transcriptomics · Wnt signaling pathway · Neuroplasticity

Introduction

Methyl donor deficiency (MDD) during pregnancy results in deleterious effects on brain development in the progeny, including the well-known neural tube defects, as well as learning and memory deficits [1]. According to the fetal programming hypothesis [2], early MDD also displays long-term effects, occurring during adolescence and later in adulthood and aging, with an increased incidence of cognitive impairments [3], and neurological diseases such as anxiety disorders, autism, or schizophrenia [4].

Metabolic consequences of MDD have been largely described in the literature [2, 5]. A deficiency in methyl donors (essentially vitamin B9, i.e., folate, and vitamin B12, i.e., cobalamin) results in the accumulation of the neurotoxic amino acid homocysteine (Hcy) along with a decrease of the S-adenosylmethionine/S-adenosylhomocysteine (SAM/SAH) *ratio*. SAM is the universal methyl group donor used for the transmethylation reactions involved in epigenomic and epigenetic regulations of gene expression, which are altered following MDD [2].

At the cellular level, the deleterious effects of early MDD are strongly related to Hcy accumulation, affecting neurogenesis and synaptic plasticity during cerebral development [2]. In an animal model based on rats born to dams fed an MDD diet during

Brigitte Leininger-Muller and Natacha Dreumont contributed equally to this work.

Electronic supplementary material The online version of this article (https://doi.org/10.1007/s12035-018-1128-3) contains supplementary material, which is available to authorized users.

✉ Brigitte Leininger-Muller
brigitte.leininger@univ-lorraine.fr

✉ Natacha Dreumont
natacha.dreumont@univ-lorraine.fr

[1] Université de Lorraine, INSERM, NGERE, F-54000 Nancy, France

[2] Present address: CALBINOTOX (EA7488), Faculté des Sciences et Techniques, Vandoeuvre lès Nancy, France

gestation and lactation [6], we reported that Hcy accumulates in the cerebellar Purkinje cells of 21-day-old (P21) rat offspring [6, 7]. We also described the hallmarks of increased apoptosis in selective brain structures of the progeny, including the pyramidal neurons of the CA1 region as well as postnatal neurogenic areas such as the hippocampal *dentate gyrus* [6, 8] and the olfactory bulbs [7]. At the functional level, the rat pups exhibited cognitive defects and an impairment of locomotor coordination [6], the young females being less efficient than the males in the cerebellum-dependent negative geotaxis behavioral test [9]. In addition to its well-known role in motor coordination, the cerebellum is also involved in cognitive tasks (attention, emotional behavior) through the coordination of the cortico-thalamic-cerebellar-cortical circuit [10]. Recent studies showed its implication in psychiatric disorders such as anxiety, autism, and schizophrenia [11]. At the molecular level, we observed a strong decrease of neurosteroidogenesis and the related cAMP-mediated signaling pathway, in association with a decreased expression of estrogen receptors [12] and of synapsins [9]. These changes occurred in a sex-dependent manner, females being more affected than males.

As pinpointed above, the cerebellum is particularly affected by an early MDD or by exposure to other environmental factors, since its maturation mainly occurs during the postnatal period and is achieved around the third postnatal week [13, 14]. The cerebellum contains relatively few cell types and its architecture is somewhat simple compared with other brain structures, with three layers composing the cerebellar cortex: the innermost granular layer, the middle Purkinje cell layer, and the outermost molecular layer. The principal cytostructure is set during early development but neurogenesis and axonogenesis take place after birth. During the first two postnatal weeks, Purkinje cells undergo maturation by developing dendritic trees and synaptic connections, and form a single cell layer. The granular cells (representing about half the number of total neurons in the brain) migrate after birth from the external granular layer (EGL) to enter the molecular layer and finally reach their final destination. Among the cellular pathways involved in postnatal cerebellum development, the Wnt pathway plays a critical role in regulating cellular growth and differentiation, allowing synapse formation and axon guidance [15, 16]. Wnt ligands are recognized by their cell surface receptors and through several cytoplasmic components, notably glycogen synthase kinase-3β (GSK3β), signal to β-catenin, which enters the nucleus and coactivates transcription of target genes to regulate cell fate decision. In addition, Wnt signaling regulates microtubule cytoskeleton through a divergent branch of this canonical pathway. Two non-canonical pathways, the planar cell polarity and the calcium pathways, are independent of GSK3β and β-catenin, and control cell polarity and regulate cell movement, respectively. Wnt family proteins do not only regulate early embryonic development. Recent evidence suggests that they also modulate synaptic development and function. In the cerebellum, Wnt-7a is expressed in granular cells when mossy fiber axons make synaptic contact with granular cells [15], thereby regulating axon remodeling and synaptic differentiation. Wnt-3a expression is more specific to Purkinje cells. It increases postnatally as granular cells start to make contacts with Purkinje cells and are restricted to these cells in the adult mouse [16].

Despite the numerous consequences of an early MDD on the development of the central nervous system, the molecular mechanisms underlying cellular response to MDD remain poorly understood, even more in the cerebellum. Here, we investigated the impact of MDD on cerebellum development in female rats (these being more affected than males) by carrying out whole transcriptome analysis, with the aim of identifying new genes and molecular pathways associated with the functional alterations previously observed [6, 9].

Materials and Methods

Animals

Experiments were performed on Wistar rats (Janvier Labs) in accordance with the National Institute of Health Guide for the Care and Use of Laboratory Animals in an accredited establishment (Institut National de la Santé et de la Recherche Médicale, Unité 1256) according to the UE guidelines 2010-63-UE and to French governmental decree 2013-118. Adult rats were maintained under standard laboratory conditions on a 12-h light/dark cycle with access to food and water ad libitum. One month before pregnancy, female rats were fed either a standard diet (A04 Standard Diet, Safe, Augy, France), or a diet deficient in folate and vitamin B12 and lowered in choline (Special Diet Service, Saint-Gratien, France). These diets were maintained until the offspring was weaned at postnatal day 21 (P21).

Tissue Collection

Rat pups were euthanized at P21 with an overdose of isoflurane. Blood samples were collected by exsanguination for the plasma biochemical measurements. Cerebellums were rapidly harvested and kept frozen in liquid nitrogen until biochemical analyses. For immunohistofluorescence analyses, brains were fixed with paraformaldehyde 4% for 24 h, washed three times in PBS 1X, dehydrated in a sucrose gradient (10 to 30%), and finally frozen in methylbutane previously chilled to − 30 °C and stored at − 80 °C.

Biochemical Analyses

Plasma concentrations of vitamins B9 and B12 were determined using a radioisotope dilution assay (simulTRAC-SNB; ICN Pharmaceuticals, Laval, France) as previously

described [6]. Concentrations of Hcy, SAM, and SAH were measured using high-performance liquid chromatography as previously described [17].

Microarray Experiment

Total RNA was extracted from 20 mg of ground cerebellum from female P21 pups (control, $N = 4$; MDD, $N = 3$) using TriZol (Invitrogen, Carlsbad, California, USA) according to the manufacturer's recommendations. RNA was further digested with Turbo DNase (Thermo Fisher, Waltham, Massachusetts, USA) and phenol-chloroform extracted. Quality of total RNAs was attested by $O.D._{260\ nm}/O.D._{280\ nm}$ and $O.D._{260\ nm}/O.D._{230\ nm}$ determination by spectrophotometry using a Nanodrop ND-1000 (NanoDrop Technologies; Wilmington, DE, USA) and using a 2100 Bioanalyzer (Agilent Technologies; Massy, France). The samples with a RNA integrity number > 8 were selected. RNA samples were aliquoted and stored at − 80 °C for subsequent microarray.

Microarray experiments were performed following the minimal information about a microarray experiment criteria [18]. Briefly, RNA samples were amplified and labeled using the one-color microarray-based gene expression labeling kit (Agilent Technologies; Massy, France) following the manufacturer's instructions. The RNA was denatured and reverse transcribed to cDNA. The cDNA was transcribed in vitro to RNA using T7 RNA polymerase and labeled with fluorescent cyanine 3-CTP. The fragmented cRNA was hybridized to a G4853A SurePrint G3 Rat GE 8X60K microarray (Agilent Technologies; Massy, France). The microarrays were performed in triplicate and washed, stabilized, and dried using acetonitrile and stabilization and drying solution (Agilent Technologies; Massy, France). The slides were scanned and the images were extracted using feature extraction software version 9.5.3 (Agilent Technologies; Massy, France).

Bioinformatic Analysis

Raw expression values were extracted from the Agilent data files. Control probes were removed and the 58,717 remaining probes were fully annotated at transcript and gene levels with up to date symbols using the local rat Ensembl database (core and funcgen 83_6) [19]. Non-linear effects such as background or saturation were corrected by the Lowess algorithm [20] against a median profile of all seven samples. Hierarchical clustering (performed with Cluster3.0 [21] was then used to identify clusters of co-expressed genes from the whole dataset, on log-transformed and gene-median-centered data, using uncentered Pearson's correlation as similarity metric. From the gene clustering tree, sets separating control ($N = 4$) and MDD ($N = 3$) samples were delineated and a collective p value (Student t test) was computed between each group, hence allowing us to dismiss multi-testing correction. For each selected gene cluster, functional annotations were obtained with GoMiner [22] on the Gene Ontology (GO) database (October 2016 version). Enrichment of GO terms was determined as follows: enrichment = frequency of GO term in the cluster/frequency of GO term in the whole chip.

Measurement of Granular Cell Layer Thickness and Purkinje Cell Counting

After 4,6-diamidino-2-phenylindole nuclear fluorescent dye (DAPI) staining, 12 μm sagittal brain sections were observed under fluorescence microscopy (BX51WI; Olympus, Tokyo, Japan) at × 20 magnification. All measurements were performed in the cerebellar VII lobule using ImageJ v1.49. The thickness of the granular layer was determined by measuring the maximum distance separating the two outermost points at the extremity of the lobule (a distance). The b distance was determined from the inside to the outside of the granular layer on the side of the lobule, forming a right angle with the greater distance a.

The number of Purkinje cells per microscope field was determined after specific staining with calbindin D28. Since this specific staining allows to clearly distinguishing the Purkinje layer from the granular and the molecular layers, some areas could be drawn with the software around several Purkinje cell bodies. This procedure was randomly repeated at least three times on each slide. Finally, the average number of Purkinje cells was reported to 1000 μm^2.

Immunohistofluorescence

Immunohistofluorescence analyses were carried out on cryostat-generated, 12 μm sagittal brain sections mounted onto glass slides. For immunostaining, tissue sections previously fixed in 4% paraformaldehyde (Sigma-Aldrich, St. Louis, Missouri, USA) for 15 min at room temperature were permeabilized for 10 min in PBS-0.1% Triton. After three washes in PBS of 5 min each, nonspecific binding was prevented by incubation in PBS-BSA 10% (w/vol) for 1 h. Tissue sections were further incubated for 48 h at 4 °C with primary antibody against Calbindin D28 (Santa Cruz Biotechnology, Dallas, Texas, USA) used at a 1:200 dilution. Brain slices were then incubated for 2 h at room temperature in the presence of the secondary antibody (Alexa Fluor 594 donkey anti-goat, Abcam, Cambridge, UK). All slides were counterstained with DAPI (0.5 mg/mL in PBS; Sigma-Aldrich, St. Louis, Missouri, USA). Slides were observed under fluorescence microscopy (BX51WI; Olympus, Tokyo, Japan) at × 20 magnification, and pictures were taken via a digital

camera and the cellF software (Soft Imaging System; Olympus, Tokyo, Japan).

Western Blot Analyses

Nitrogen-frozen cerebellum samples were solubilized in RIPA lysis buffer containing 140 mM NaCl, 0.5% (*w*/*v*) sodium deoxycholate, 1% (*v*/*v*) Igepal CA630 (Sigma-Aldrich, St. Louis, Missouri, USA), 0.1% (*w*/*v*) sodium dodecyl sulfate, and protease inhibitors (Sigma-Aldrich, St. Louis, Missouri, USA). Samples were then homogenized in a ultrasonic bath during 30 min and finally centrifuged at 4 °C for 30 min at 18,000*g*.

Thirty micrograms of proteins were mixed with an equal volume of 2X Laemmli buffer, denatured by heating for 5 min at 95 °C, and then resolved by 10% SDS-PAGE. The separated proteins were then transferred onto nitrocellulose membrane (GE healthcare Life Sciences, Marlborough, Massachusetts, USA) and blocked for 1 h under shaking with Tris-buffered Saline solution (20 mM Tris and 150 mM NaCl, pH = 7.4) and 0.1% Tween-20 containing 5% (*w*/*v*) bovine serum albumin. The membranes were finally incubated with different primary antibodies at 4 °C overnight: CamkII (Gentex, Zeeland, Michigan, USA), Ccd1 (Proteintech, Rosemont, Illinois, USA), c-myc and P300 (Santa Cruz Biotechnologies, Dallas, Texas, USA), β-catenin, cyclin D1, GSK-3β, JNK and phospho-JNK (Cell Signaling Technology, Danvers, Massachussetts, USA); GAPDH and Gria2 (Abcam, Cambridge, UK), vinculin (Merck, Darmstadt, Germany). Secondary peroxidase-labeled antibodies (Jackson Immunoresearch Laboratories, West Grove, Pennsylvania, USA) were used at a 1:10,000 dilution and were incubated with the membranes for 1 h at room temperature. Immunoreactivity was detected with a chemiluminescence kit (ECL Plus, GE healthcare Life Sciences, Marlborough, Massachusetts, USA) and a chemiluminescence detector (Fusion FX7; Thermo Fisher, Waltham, Massachusetts, USA). The total amount of proteins per lane was normalized using GAPDH or vinculin antibody (Table 1) and densitometric analysis of the Western blot band intensity was achieved using ImageJ v1.49.

Quantitative RT-PCR Analysis

One microgram of total RNA was subjected to 2-step RT-qPCR using the PrimeScript™ RT Master Mix and SYBR® Premix Ex Taq™ (Takara, Kusatsu, Japan) following the manufacturer's specifications. Primers were ordered from Biorad, Hercules, California, USA (PrimePCR™ SYBR® Green Assay). Cycle threshold (Ct) was determined for each sample and real-time PCR amplification efficiencies were expressed by calculating the *ratio* of crossing points of amplification curves. The expression of the genes of interest was normalized to those of *gapdh* and *kansl2* using the 2-ΔΔCt method.

Determination of Free Intracellular Calcium

Free intracellular calcium concentration was measured with Calcium Detection Kit Colorimetric (Abcam, Cambridge, UK). Twenty milligrams of ground cerebellum was lyzed on ice in calcium assay buffer. After 3 min of centrifugation at 10,000*g* and 4 °C, supernatants were collected and 50 μL of each sample was deposited in a 96-well plate. Ninety microliters of chromogenic reagent and 90 μL of calcium assay buffer were added to each sample as recommended by the manufacturer. A standard curve was performed in parallel with calcium standard and O.D. was finally measured at 575 nm.

Statistical Analyses

Statistical analyses were performed under RStudio, version 1.0.143. Continuous variables and densitometric analyses of Western blots were reported as means ± SD. Equality of variances was checked by Fisher's test. Differences between control and MDD groups were assessed with the Student *t* test. A p value < 0.05 was considered to indicate statistical significance.

Results

SAM/SAH Ratio and Vitamins B9 and B12 Concentrations

As previously described, when female pups were fed by dams receiving the deficient diet, plasma levels of vitamins B9 and

Table 1 Effects of the diet on plasma concentrations of homocysteine and its determinants in 21-day-old female rat progeny

	B9 (nM)	B12 (pM)	Hcy (μM)	SAM (nM)	SAH (nM)	SAM/SAH
Control	48.8 ± 3.5	841.8 ± 17.2	6.50 ± 0.88	440.2 ± 29.3	84.2 ± 6.8	5.27 ± 0.33
MDD	20.1 ± 2.8*	262.2 ± 12.4*	13.86 ± 2.67*	390 ± 20.3	135.6 ± 17.1*	3.31 ± 0.36*

Data are means ± SEM, $N = 11$ per group, $^*p \leq 0.05$

Hcy, homocysteine; Met, methionine; SAM, *S*-adenosylmethionine; SAH, *S*-adenosylhomocysteine

B12 were reduced compared to controls, with a concomitant increase of Hcy levels (Table 1). The universal methyl donor SAM, generated through the methionine cycle, is demethylated to form SAH, which is finally hydrolyzed into Hcy. SAM concentration remained unchanged whereas SAH concentration was higher in MDD compared to control females (Table 1). The SAM/SAH *ratio* was therefore lower in deficient females compared to controls (Table 1).

Transcriptomic Analysis of Early MDD Effects on the Female Rat Cerebellum

The comparison of the whole transcriptomes, measured by the 58,717 probes constituting the microarray and corresponding to 30,584 transcripts, was done by applying hierarchical clustering, which separated both control and MDD groups distinctly (Fig. 1). In addition, three gene signatures with highly correlated expression profiles were delineated (Fig. 1). The first one comprised 1875 unique genes (cluster C1) that are upregulated in MDD ($p < 0.05$). The two others contained respectively 1144 (cluster C2) and 602 (cluster C3) unique genes, downregulated in MDD vs controls ($p < 0.05$; Fig. 1).

Functional annotations revealed that upregulated C1 genes, in addition to glutathione metabolism, ribosome, and translation, were mostly related to mitochondria, with functions such as proton transport coupled to ATP synthesis, oxidative phosphorylation, and respiratory chain IV complex assembly (FDRs < 0.001; Table 2). In contrast, downregulated genes in clusters C2 and C3 were related to cerebellum development (mostly in C2), synaptic plasticity (mostly in C3), and regulation of neurotransmitter release (FDRs < 0.001; Tables 3 and 4). We also identified functional terms related to RNA pol II coactivator activity and histone demethylation in C2, and to poly(A) RNA binding in C3 (FDRs < 0.001; Tables 3 and 4).

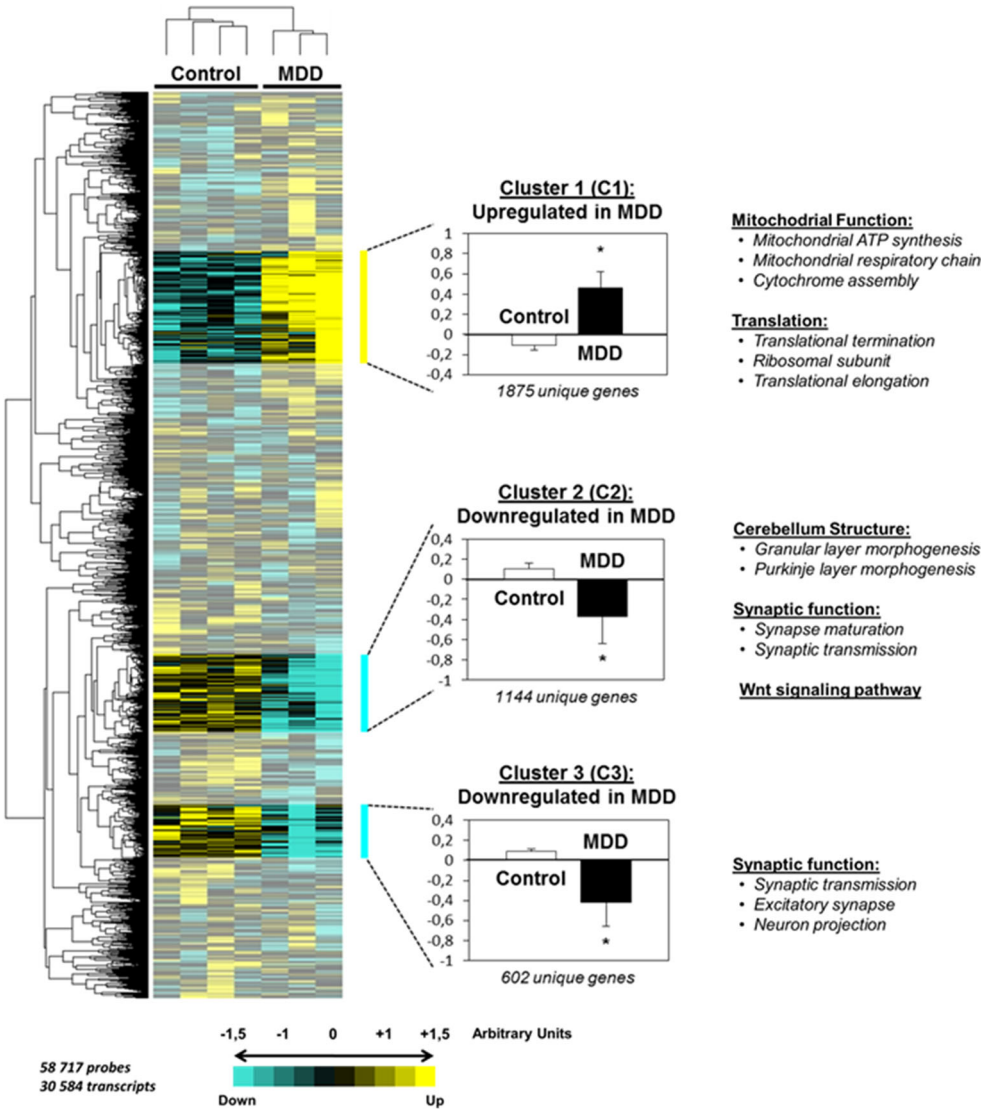

Fig. 1 Consequences of MDD diet on the cerebellum transcriptome of 21-day-old female rats. Hierarchical clustering of the whole transcriptome uncovered three significant gene signatures. Left panel: Heatmap with gene and sample trees. Gene expression is presented as a colored matrix (blue: downregulated genes; yellow: upregulated genes; black: median genes). Right panels: Overall differential expression for each cluster of co-expressed genes. Expression values are log2-centered. Some of the functions that are dysregulated in MDD are indicated

Table 2 Most enriched functional terms for the upregulated gene signature C1 in the cerebellum of female rat progeny subjected to methyl donor deficiency (FDRs were obtained by bootstrapping 50 times)

GO ID	Total	Change	Enrichment	*p* value	FDR	Term
6558	12	8	5.952	0	0	L-Phenylalanine metabolic process
70129	14	8	5.102	0	0.0011	Regulation of mitochondrial translation
42776	14	8	5.102	0	0.0011	Mitochondrial ATP synthesis coupled proton transport
33617	14	8	5.102	0	0.0011	Mitochondrial respiratory chain complex IV assembly
1901685	16	9	5.022	0	8.00E-04	Glutathione derivative metabolic process
313	85	40	4.201	0	0	Organellar ribosome
5761	78	36	4.121	0	0	Mitochondrial ribosome
70124	64	28	3.906	0	0	Mitochondrial translational initiation
70126	69	30	3.882	0	0	Mitochondrial translational termination
17004	28	12	3.826	0	0.0012	Cytochrome complex assembly
70125	73	30	3.669	0	0	Mitochondrial translational elongation
6415	79	32	3.616	0	0	Translational termination
44391	120	47	3.497	0	0	Ribosomal subunit
2479	44	16	3.246	0	0	Antigen processing and presentation of exogenous peptide antigen via MHC class I, TAP-dependent
6414	95	34	3.195	0	0	Translational elongation
5840	160	57	3.181	0	0	Ribosome
33108	62	21	3.024	0	0	Mitochondrial respiratory chain complex assembly
6614	54	18	2.976	0	8.00E-04	SRP-dependent cotranslational protein targeting to membrane
45047	59	19	2.875	0	8.00E-04	Protein targeting to ER
51439	50	16	2.857	1.00E-04	0.0017	Regulation of ubiquitin-protein ligase activity involved in mitotic cell cycle
5746	50	16	2.857	1.00E-04	0.0017	Mitochondrial respiratory chain
6119	81	22	2.425	1.00E-04	0.001	Oxidative phosphorylation

Methyl Donor Deficiency Reduces the Granular Cell Layer Thickness and the Number of Purkinje Cells

Interestingly, among the top hits of downregulated functions in MDD females, we found granular and Purkinje cell layer formation (GO IDs 21684 and 21692; FDRs < 0.001; Table 4), suggesting that the cytoarchitecture of the cerebellum could be affected by MDD. We therefore measured the thickness of the granular cell layer in lobule VII (Fig. 2a), at folium surface (distance *a*; Fig. 2a) and on both sides facing at fissure (distance *b*; Fig. 2a). The thickness was significantly reduced in P21 female MDD pups compared to age-matched control females, for both measurements (Fig. 2b). Similarly, the number of Purkinje cells, visualized by a specific staining with the calbindin D28 marker (Fig. 2c), was also decreased in MDD compared to control females (about twofold; $p < 0.05$; Fig. 2d).

Methyl Donor Deficiency Affects the Wnt Canonical Pathway

In addition to cerebellum development, many GO terms for the downregulated genes in MDD were related to synaptic functions (Tables 3 and 4). Moreover, Wnt signaling pathway (GO ID 160055, FDR < 0.005; Table 3) was also identified among these terms. We further investigated this important pathway, as both canonical and non-canonical pathways play key roles in neuronal connectivity by regulating axon guidance, dendritic development, axon remodeling, and synapse formation [23].

We first assessed the expression level of two ligand proteins, Wnt-3a and Wnt-7a, known to be expressed in the Purkinje and the granular cells, respectively. Western blot analyses revealed no change in the expression level of Wnt-7a or Wnt-3a (Fig. 3a) between MDD and control pups. However, we observed a twofold increase of GSK-3β, and a concomitant decrease of β-catenin levels in cerebellum extracts from MDD females compared to controls (Fig. 3b). These two proteins are key regulators of the canonical pathway, as GSK3-β regulates the degradation of β-catenin, which after translocation in the nucleus forms the β-catenin T cell factor (TCF) transcription complex that activates the expression of target genes. Indeed, we observed a twofold decrease in the level of MYC and cyclin D1 proteins (Fig. 3b), and a reduced expression of NeuroD1 (Supplementary Fig. 1), three major targets of the Wnt canonical pathway.

Table 3 Most enriched functional terms for the downregulated gene signature C2 in the cerebellum of female rat progeny subjected to methyl donor deficiency (FDRs were obtained by bootstrapping 50 times)

GO ID	Total	Change	Enrichment	*p* value	FDR	Term
1904861	9	6	8.505	0	3.00E-04	Excitatory synapse assembly
97470	9	6	8.505	0	3.00E-04	Ribbon synapse
90129	8	5	7.974	1.00E-04	0.0019	Positive regulation of synapse maturation
97119	10	6	7.655	0	9.00E-04	Postsynaptic density protein 95 clustering
32239	11	6	6.959	1.00E-04	0.0011	Regulation of nucleobase-containing compound transport
70571	12	6	6.379	1.00E-04	0.0019	Negative regulation of neuron projection regeneration
21683	15	7	5.954	1.00E-04	0.0011	Cerebellar granular layer morphogenesis
32452	18	8	5.670	0	7.00E-04	Histone demethylase activity
21692	19	8	5.372	0	8.00E-04	Cerebellar Purkinje cell layer morphogenesis
70076	17	7	5.253	2.00E-04	0.0019	Histone lysine demethylation
21681	17	7	5.253	2.00E-04	0.0019	Cerebellar granular layer development
21697	29	11	4.839	0	3.00E-04	Cerebellar cortex formation
21533	30	11	4.678	0	3.00E-04	Cell differentiation in hindbrain
1105	33	12	4.639	0	4.00E-04	RNA polymerase II transcription coactivator activity
35371	22	8	4.639	2.00E-04	0.002	Microtubule plus-end
21587	46	16	4.438	0	0	Cerebellum morphogenesis
98815	33	11	4.253	0	7.00E-04	Modulation of excitatory postsynaptic potential
21575	54	16	3.780	0	0	Hindbrain morphogenesis
35176	52	15	3.680	0	3.00E-04	Social behavior
2000171	35	10	3.645	3.00E-04	0.0045	Negative regulation of dendrite development
45773	46	12	3.328	2.00E-04	0.002	Positive regulation of axon extension
60079	59	15	3.244	0	7.00E-04	Excitatory postsynaptic potential
99565	69	16	2.958	1.00E-04	0.0011	Chemical synaptic transmission. Postsynaptic
60078	70	16	2.916	1.00E-04	0.0013	Regulation of postsynaptic membrane potential
35249	68	15	2.814	2.00E-04	0.0031	Synaptic transmission, glutamatergic
21549	126	27	2.734	0	0	Cerebellum development
51899	75	16	2.722	2.00E-04	0.0029	Membrane depolarization
7269	129	27	2.670	0	0	Neurotransmitter secretion
99531	135	28	2.646	0	0	Presynaptic process involved in chemical synaptic transmission
60076	193	40	2.644	0	0	Excitatory synapse
14069	175	36	2.624	0	0	Postsynaptic density
1505	171	35	2.611	0	0	Regulation of neurotransmitter levels
99572	176	36	2.610	0	0	Postsynaptic specialization
97060	147	30	2.604	0	0	Synaptic membrane
50773	148	28	2.414	0	3.00E-04	Regulation of dendrite development
7626	269	44	2.087	0	0	Locomotory behavior
16358	273	44	2.056	0	4.00E-04	Dendrite development
45666	350	56	2.041	0	0	Positive regulation of neuron differentiation
43087	193	30	1.983	2.00E-04	0.0032	Regulation of GTPase activity
16055	415	53	1.629	3.00E-04	0.0047	Wnt signaling pathway

About 100 target genes for the Wnt canonical pathway are described and experimentally validated (listed at https://web.stanford.edu/group/nusselab/cgi-bin/wnt/target_genes). They are mostly involved in development and cancer. These genes were not significantly enriched among the differentially expressed genes in the MDD rats compared to controls (Table 5). However many of them are not neuron-specific. We therefore took advantage of a list of 428 rat genes considered putative targets of the Wnt canonical pathway established by Wisniewska et al. [24]. Among these 428 target genes, 358

Table 4 Most enriched functional terms for the downregulated gene signature C3 in the cerebellum of female rat progeny subjected to methyl donor deficiency (FDRs were obtained by bootstrapping 50 times)

GO ID	Total	Change	Enrichment	*p* value	FDR	Term
7270	126	18	3.471	0	0.0031	Neuron-neuron synaptic ransmission
14069	175	22	3.055	0	0	Postsynaptic density
99572	176	22	3.037	0	0.004	Postsynaptic specialization
60076	193	24	3.022	0	0	Excitatory synapse
44306	187	23	2.989	0	0	Neuron projection terminus
44456	471	43	2.218	0	0	Synapse part
45202	611	54	2.148	0	0	Synapse
99537	524	45	2.087	0	0	Trans-synaptic signaling
99536	524	45	2.087	0	0	Synaptic signaling
98916	524	45	2.087	0	0	Anterograde trans-synaptic signaling
7268	524	45	2.087	0	0	Chemical synaptic transmission
44822	908	66	1.766	0	0.0036	Poly(A) RNA binding
97458	1251	84	1.632	0	0.0033	Neuron part

were expressed in our microarray experiment and were significantly enriched (p value < 0.05, Fisher's exact test, Table 5; Supplementary Fig. 1) in the downregulated signatures C2 and C3. When looking at the 38 neuronal targets (some of them being experimentally validated), we observed a 42% enrichment in the down signatures. General functional annotations for these Wnt target genes were related to neurogenesis and synaptic plasticity (voltage-gate cation channels,

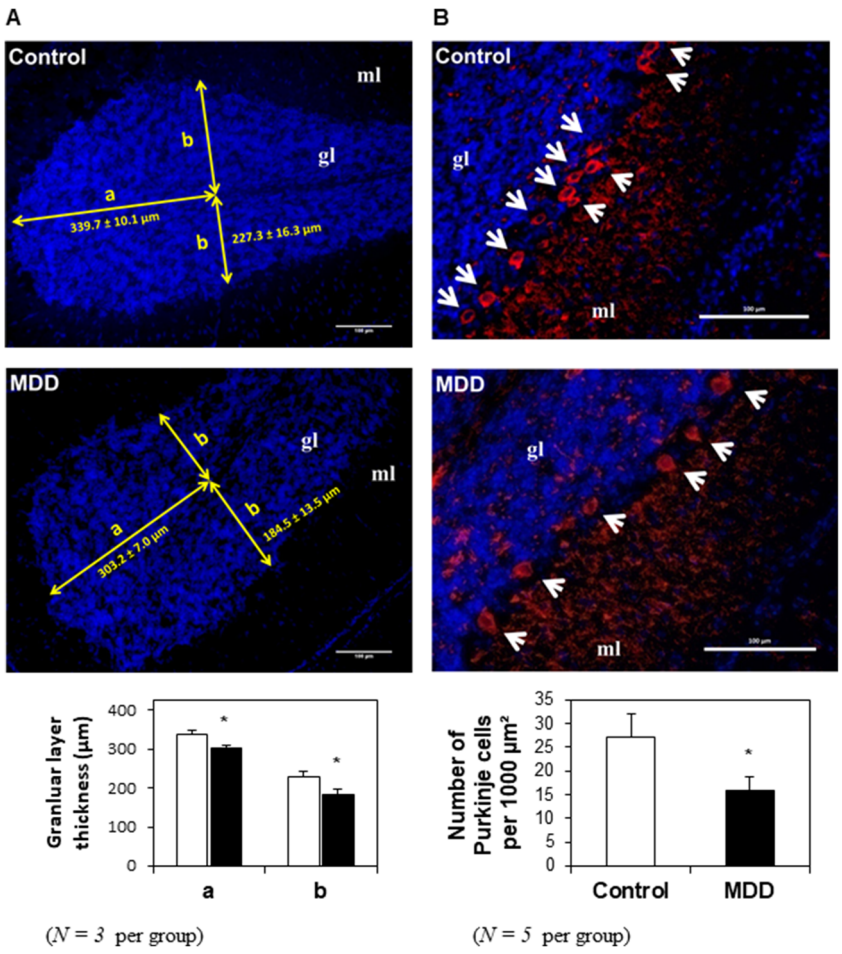

Fig. 2 MDD affects cerebellum cytoarchitecture. **a** Granular layer thickness was measured on midsagittal sections of cerebellum at folium surface (**a**) and laterally facing the fissure (**b**) in control (white bars) and MDD (black bars) females at P21. $N = 3$ per group, $^*p \leq 0.05$. **b** Specific staining with calbindin D28 to count the number of Purkinje cells per 1000 µm^2 in control (white bars) and MDD (black bars) female cerebellum at P21. $N = 5$ per group, $^*p \leq 0.05$. gl: granular layer; ml: molecular layer

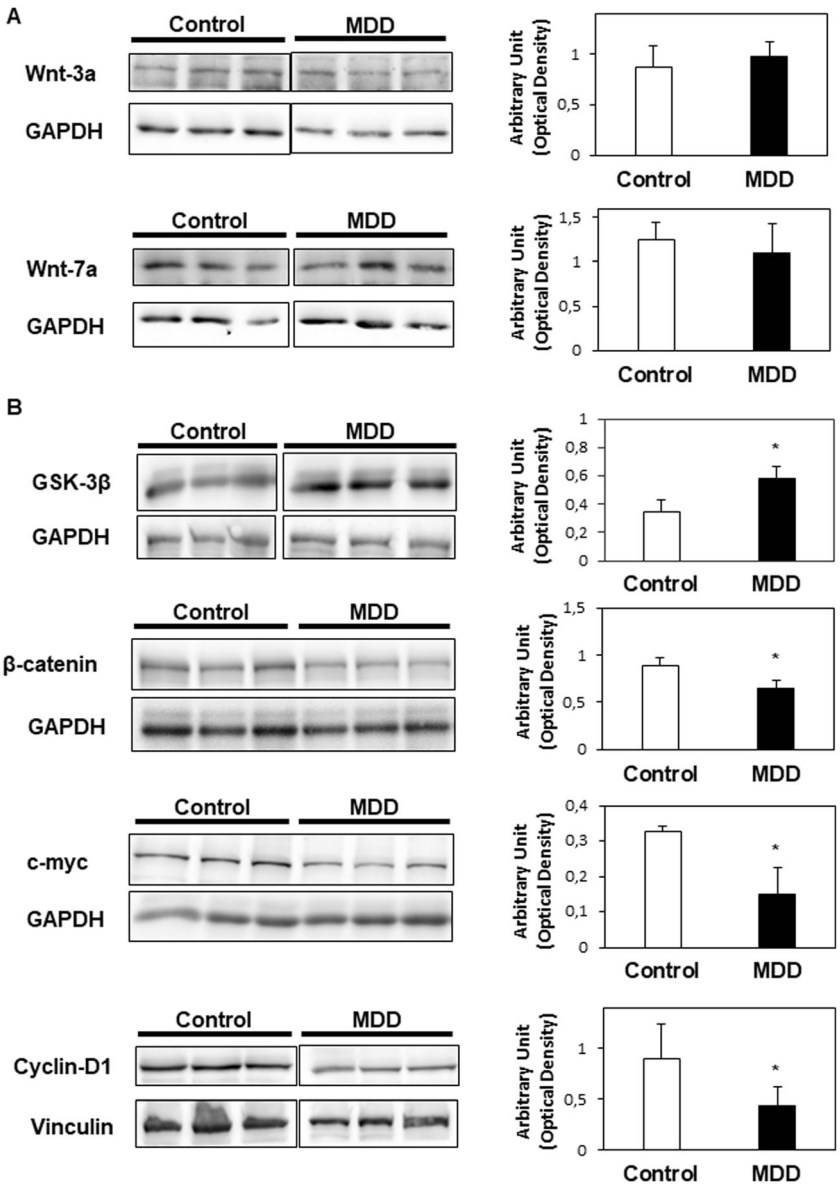

Fig. 3 The canonical Wnt pathway is downregulated in response to MDD in female's cerebellum at postnatal day 21. Western blot analysis of the expression of **a** Wnt-3a, Wnt-7a, **b** GSK-3β (glycogen synthase kinase 3 beta), β-catenin, c-myc, cyclin-D1 and densitometric quantifications of relative expressions. Arbitrary units ± SD, $N = 3$ per group, run in duplicate, $^{*}p \leq 0.05$

neurotransmitter receptor, synaptic vesicle proteins, and structural synaptic proteins), terms also identified as downregulated in our microarray experiment (Tables 3 and 4). We experimentally validated some of these target genes by measuring their expression by RT-qPCR and found that most of them were indeed strongly downregulated in MDD female cerebellum (Supplementary Fig. 1).

Wnt signaling has also been shown to regulate cytoskeleton through a divergent canonical pathway, independent of TCF-mediated transcription. In this case, GSK-3β phosphorylates microtubule-associated proteins such as MAP1B [25]. In agreement with the increased level of GSK-3β (Fig. 3b), we observed more phosphorylated MAP1B in MDD females compared to controls (Fig. 5b).

Taken all together, these data show a dysregulation of the Wnt canonical pathway in response to MDD in female cerebellum at P21, which could result in altered synaptic functions.

Methyl Donor Deficiency May Affect the Wnt-Ca^{2+} Pathway but not the PCP Pathway

Independently of β-catenin, non-canonical Wnt pathways have been described: the planar cell polarity (PCP) and the Wnt-Ca^{2+} pathways. In addition to cell fate, tissue polarity and cell movement, these were shown to be involved in dendritogenesis and regulation of postsynaptic region [26]. We therefore asked whether these pathways were

Table 5 Putative and verified target genes of the Wnt canonical pathway are enriched in the downregulated signatures C2 and C3

Targets or functional lists	Genes expressed on microarray	Downregulated signatures (C2+C3)	Relative enrichment (C2+C3)	Upregulated signature (C1)	Relative enrichment (C1)	Distribution bias (p-value)	Heat map (ref)
Known Beta-Catenin targets (not neural specific)	**81**	**5 (6.2%)**	**0.65**	**5 (6.2%)**	**0.58**	0.26	
Gliogenesis	**9**	**1 (11.1%)**	**1.16**	**3 (33.3%)**	**3.11**	8.28E-02	**A**
Neurogenesis	**76**	**17 (22.4%)**	**2.34**	**9 (11.8%)**	**1.1**	**1.97E-03**	
Regulation of neurogenesis	**13**	**3 (23.1%)**	**2.41**	**0 (0%)**	**0**	0.15	**B**
Putative LEF1/TCF targets (computationally predicted by TFBS motif enrichment)	**358**	**46 (12.8%)**	**1.34**	**29 (8.1%)**	**0.75**	**4.79E-02**	
Predicted and verified targets involved in neuronal signal transmission	**38**	**16 (42.1%)**	**4.4**	**1 (2.6%)**	**0.25**	**3.05E-07**	
Voltage gate cation channels (VGCC)	**9**	**4 (44.4%)**	**4.65**	**0 (0%)**	**0**	**1.34E-02**	**C**
Neurotransmitter receptors	**9**	**3 (33.3%)**	**3.49**	**0 (0%)**	**0**	6.37E-02	
Synaptic vesicle proteins	**8**	**2 (25%)**	**2.61**	**0 (0%)**	**0**	0.27	
Structural synaptic proteins	**9**	**7 (77.8%)**	**8.13**	**1 (11.1%)**	**1.04**	**1.22E-06**	
SNV development	**20**	**7 (35%)**	**3.66**	**0 (0%)**	**0**	**1.95E-03**	**D**
Axon guidance	**19**	**4 (21.1%)**	**2.2**	**0 (0%)**	**0**	7.89E-02	**E**
Long term synaptic plasticity	**23**	**7 (30.4%)**	**3.18**	**2 (8.7%)**	**0.81**	**9.12E-03**	**F**
Neural cell body	**36**	**12 (33.3%)**	**3.49**	**0 (0%)**	**0**	**4.75E-05**	**G**

Functional lists were obtained and compiled from Wisniewska et al. [24] and MSigDB curated gene sets. Statistical significance for signature enrichments is indicated in the distr ibution bias column (Fisher's exact test, two-sided, a p value < 0.05 is considered as significant). Hierarchical clustering heat maps are also available in Supplementary Fig. 1 (A to G).

also dysregulated, in addition to the Wnt canonical signaling pathway.

The Wnt/PCP pathway is activated by the binding of Wnt proteins to their receptor, resulting in the activation of the small GTPases Rho and Rac, and finally the activation of the c-Jun N-terminal kinase (JNK). For this reason, we evaluated the expression level in cerebellum extracts from MDD and control females of the active (phosphorylated) form of the axon-growth promoting protein kinase JNK. As shown in Fig. 4a, we did not observe any change in the phosphorylated JNK level in MDD compared to control females, suggesting that the PCP pathway was not affected by the deficiency. We also tested the expression level of *Ccd1*, which codes for an actin-binding protein, and was reported to positively regulate the Wnt signaling pathway [27] and to activate JNK, thereby promoting axonal growth and parallel fiber development [28]. *Ccd1* was one of the underexpressed genes in cluster C2, and thus found in several of the downregulated GO functional families related to neuron projection in MDD females (Table 3). As measured by RT-qPCR, the expression level of *Ccd1* was reduced in MDD females (Fig. 4b). This was in agreement with the decreased expression level of P300, the transcriptional coactivator of *Ccd1* (Fig. 4c). However, the expression of the CCD1 protein remained unchanged between MDD and control females (Fig. 4d).

Contrary to the PCP pathway, the Wnt-Ca^{2+} signaling pathway might be affected by MDD, as we measured a significantly decreased intracellular Ca^{2+} concentration in the MDD female cerebellum (Fig. 5a). This was in agreement with the previously reported diminution of phosphorylated PKC level in MDD female cerebellum [12]. Surprisingly, the level of CaMKII, a Ca^{2+}/Calmodulin-dependent kinase, was elevated in MDD compared to control females (Fig. 5c). Interestingly, levels of one subunit of the glutamatergic AMPA receptors that are present at the postsynaptic density were reduced in MDD compared to control females, suggesting alterations at the postsynaptic level (Fig. 5d).

Discussion

Reduced intake of methyl donor nutrients (essentially vitamins B9 and B12) has been implicated in alterations of neurodevelopment, as well as in several neurological and

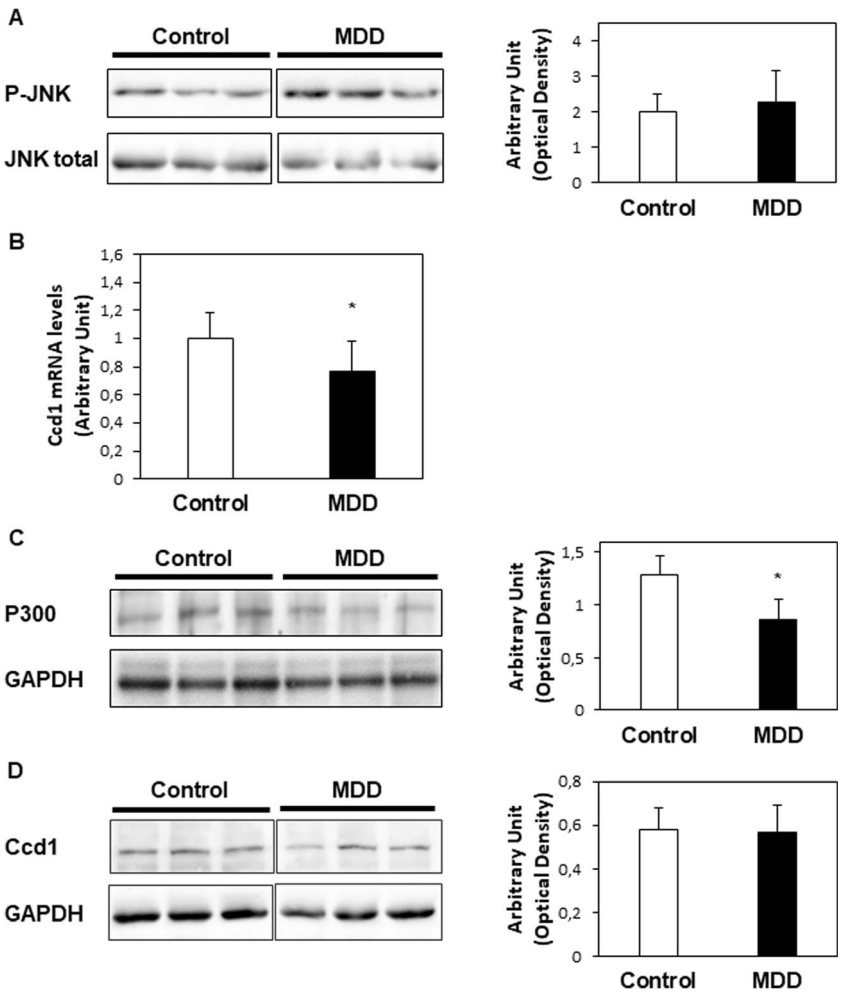

Fig. 4 MDD effects on Wnt PCP pathway in female's cerebellum at postnatal day 21. Western blot analysis of the expression of **a** phosphorylated JNK (c-Jun N-terminal kinase), **c** P300 and **d** Ccd1 (coiled-coil protein DIX1) and densitometric quantifications of relative expressions. **b** mRNA expression level of Ccd1, measured by qRT-PCR. Arbitrary units ± SD, $N = 3$ per group, run in duplicate, $^*p \leq 0.05$

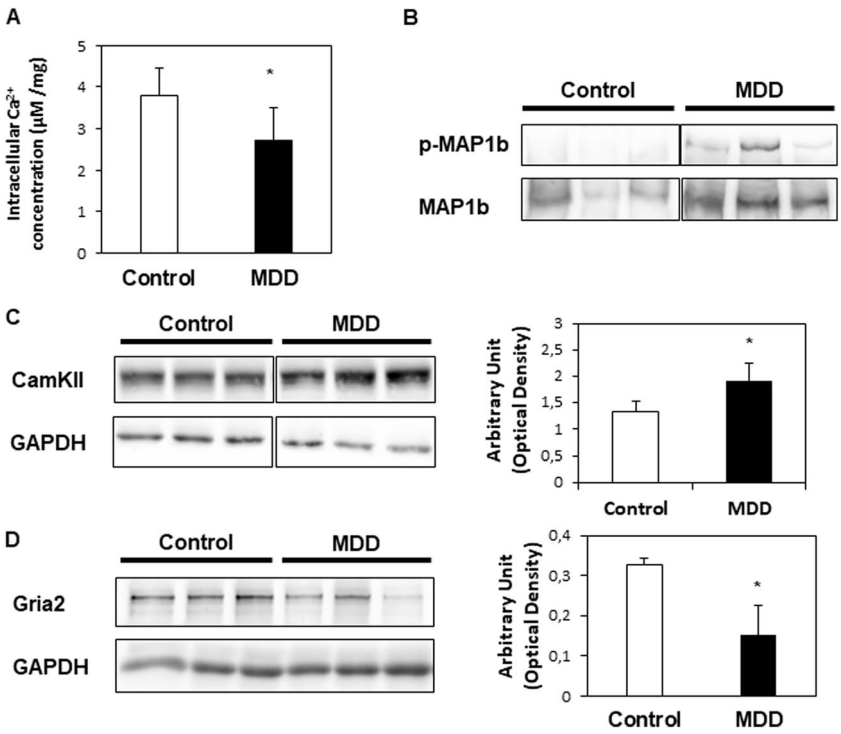

Fig. 5 MDD effects on Wnt Ca^{2+} pathway in female's cerebellum at postnatal day 21. **a** Free intracellular Ca^{2+} concentration in 21-day-old female's cerebellum in response to MDD in µM per mg of cerebellum tissue. $N = 6$ per group, $*p \leq 0.05$.Western blot analysis of the expression of **b** phosphorylated and total MAP1b, **c** CaMKII (Ca^{2+}/calmodulin-dependent protein kinase II), **d** Gria2 (glutamate ionotropic receptor AMPA type subunit 2) and densitometric quantifications of relative expressions. Arbitrary units ± SD, $N = 3$ per group, run in duplicate, $*p \leq 0.05$

psychological diseases, albeit the underlying mechanisms remain poorly understood. Our study showed that the Wnt canonical and likely the Wnt-Ca^{2+} pathways are dysregulated in female cerebellum at P21, following maternal exposure to vitamins B9 and B12 deficiency, likely contributing to the defects observed in synaptic assembly and signaling at the transcriptome level.

Functional alterations discovered so far in the brain of female pups born to dams fed a diet deficient in vitamins B9 and B12 affect mainly the hippocampus and the cerebellum. Notably, Hcy accumulates predominantly in the granular layer and in Purkinje cells [6, 12]. Previous studies in our laboratory demonstrated impaired locomotor coordination in pups exposed to the deficient diet [6]. Nevertheless, this disability appeared to be transient, suggesting a developmental retardation involving gene expression and cellular pathway downregulation [9, 12]. These observations indicate that the cerebellum is particularly sensitive to MDD during the fetal period and early after birth.

In order to identify new genes and pathways potentially involved in the functional alterations observed in the cerebellum following MDD, we performed a transcriptional analysis at P21, at the time when the cerebellum is ending its maturation. The cerebellum undergoes several major structural transformations during embryonic development, and by embryonic day 18.5, it has acquired its three-dimensional architecture. At birth, a rudimentary set of synaptic connections has begun to become organized, and the cerebellum has established all its cell types in three layers around P16 in rodents [13]. The granular cell layer forms postnatally as cells from the EGL, present at the cerebellar surface, seed the internal (and final) granular layer. The EGL ceases to exist by the end of the third postnatal week. At this period, two major extrinsic inputs to the cerebellar cortex mature with the climbing fibers connecting to the Purkinje cells and the mossy fibers to the granule cells [29]. These are the major excitatory cell types found in the cerebellum, all using glutamate as their neurotransmitter. Several genes coding for subunits of ionotropic glutamate receptors (kainate, delta, and AMPA) displayed a decreased expression in the MDD female cerebellum (Supplementary Fig. 1 and Fig. 5d), in line with an impaired synaptic plasticity, as suggested by many GO terms found in the transcriptomic analysis and previous results obtained in our laboratory [9].

Wnt signaling plays a major role in axon pathfinding, dendritic development, synapse assembly, and modulation of synaptic transmission in the central nervous system [30]. Results from the transcriptomic analysis indicated that Wnt signaling pathway was globally downregulated in MDD females, as well as the expression of many of its target genes in neurons (Table 5). Indeed, by western blot analyses, we observed that GSK3β protein level was increased in the cerebellum of MDD female pups compared to controls, resulting in a subsequent reduction of β-catenin levels, and a decreased expression of well-known target genes of the Wnt canonical signaling pathway involved in cell proliferation (c-Myc and cyclin D1, Fig. 3). This could result in decreased cell proliferation, accounting for the observed reduced thickness of the granular cell layer and the decreased number of Purkinje cells in the cerebellum of MDD pups (Fig. 2), in agreement with the downregulated

functions identified by transcriptomics (Table 3). There exists a tight regulation of the *ratio* of Purkinje cells to granule cells, with the number of Purkinje cells determining the size of the granule cell population [13]. According to this, our observations suggest that the reduced number of Purkinje cells could be the primary event, resulting in the reduced size of the granular cell layer. Apoptosis is probably not involved in this process, as we previously did not observe any difference in the cerebellum using an apoptosis marker (apostain) in MDD female pups compared to controls [9].

In addition to its role in regulating the availability of β-catenin, GSK3β directly phosphorylates several microtubule-associated proteins, such as Tau or MAP1B [25]. This role of Wnt signaling in modulating microtubule cytoskeleton could contribute to synaptic assembly and glomerular rosette assembly in particular. Indeed, following GSK3β increased expression in the cerebellum of MDD females, we detected an increased phosphorylation of MAP1B. This could result in a reduction of the formation of microtubule loops within the growth cone, and a less efficient growth cone pausing and enlargement [31]; contributing to the disruption of excitatory synapse assembly, as indicated by the transcriptomics. In addition, it was shown that Wnt could also regulate microtubule stability through JNK. However, we did not detect any change in the level of activated (phosphorylated) JNK between control and MDD pups. We also investigated the expression level of the actin-binding protein Ccd1, which was identified in many of the GO terms related to the synapse (Table 3). This protein was reported to activate JNK and play an essential role in parallel fiber development [28]. Despite a reduced expression level of its coactivator P300 and a resulting diminished mRNA expression level, Ccd1 protein expression was not affected by the restrictive diet, suggesting (i) a posttranscriptional regulation of *Ccd1*expression, and (ii) that JNK pathway is globally not affected by MDD at P21.

Wnt-7a, when released by granule cells, acts on mossy fibers to promote the formation of the glomerular rosette, the accumulation of synaptic components, such as synapsin 1 (Syn1) to future presynaptic sites [32], and synaptic vesicle recycling [33], through the canonical pathway and GSK3β. Syn1 is involved in synaptogenesis, axonogenesis and the modulation of neurotransmitter release, and associates with the cytoplasmic surface of presynaptic vesicles. Interestingly, we previously reported a decrease of Syn1 level in the cerebellum of MDD females at P21 [9]. We showed that this was due to a disruption of the ERα signaling pathway, resulting in a decreased expression of Egr1, the transcription factor regulating Syn1 [9]. Our present results suggest that in addition to ERα, Wnt canonical signaling pathway could also participate to the regulation of Syn1 expression, as Wnt-7a was reported to increase Syn1 level in cultured granule cells, an effect mediated through GSK3β [25].

At postsynaptic level, Wnt signaling promotes the recruitment of postsynaptic components, with an increased clustering of the scaffold protein PSD95 [34], a marker of postsynaptic activity involved in signal transduction of excitatory receptors. PSD95 levels are reduced in cerebellum protein extracts from females exposed to MDD [9]. We also observed less Gria2 protein, a subunit of the glutamatergic AMPA receptors that are present at the postsynaptic density, as well as a reduced expression of Gria3 mRNA (Supplementary Fig. 1). These observations could be due to the altered Wnt/Ca^{2+} signaling originating from a reduced Ca^{2+} tissue content, a decreased activation of PKC [12], and a decreased expression of transcription factors such as P300 (our present results) or CREB [12], or the downregulation of Wnt canonical pathway in the case of Gria3. In addition, the expression of many putative target genes of the Wnt canonical pathway, with functions in nervous system development or synaptic functions, was also affected by MDD (Table 5, Supplementary Fig. 1).

The dysregulation of Wnt canonical pathways is not caused by a reduced level of either Wnt-7a or Wnt-3a, which are expressed in granular cells and Purkinje cells, respectively. The link between MDD and Wnt could be at the epigenetic or epigenomic level, as MDD is known to alter gene expression through these processes [2]. Indeed, folate is required for the synthesis of SAM, which is used for DNA methylation at CpG sites. Folate deficiency is known to affect DNA methylation [35]. Inversely, gestational folate supplementation was also shown to influence the epigenome in mouse offspring cerebellum and therefore gene expression [36]. SAM is also required for methylation of histone proteins and MDD was reported to alter some histone marks such as H4K20me3 [37]. Finally, the expression of some miRNAs is dysregulated in the offspring following a gestational deficiency in vitamins B9 and B12, resulting in altered signaling pathways with key regulating functions in brain [38]. Any disruption in these epigenetic mechanisms could contribute to the altered expression of GSK3β, with the subsequent dysregulation of the Wnt canonical pathway.

In addition to impairment of cerebellum development and synaptic plasticity, transcriptomic results revealed alterations in mitochondrial functions. Notably, genes related to functional terms such as cytochrome complex, oxidative phosphorylation, ATP synthesis coupled proton transport and respiratory chain were found to be upregulated in MDD female progeny (Table 2). These results are in agreement with those previously found in the liver using the same animal model [39]. Our results suggest that the upregulation of genes involved in mitochondrial functions could be a way to compensate and to restore proper mitochondrial function. Indeed, neurons are highly dependent on mitochondrial ATP, in particular to sustain synaptic vesicle trafficking and maintenance of ion gradients across the cellular membrane. Moreover, terms such as glutathione derivative metabolic process are also associated

with an upregulation, suggesting that cells are subjected to oxidative stress. Altogether, mitochondrial dysfunction is likely to contribute to the alterations observed in the cerebellum.

Studies from human populations and experimental models suggest a role for MDD in the development of several neurodegenerative diseases, such as Parkinson disease, and also for psychiatric disorders, for example depression, bipolar disorder or schizophrenia [4]. This association between MDD and these diseases could be due in part to an increased GSK3β that is itself linked to the same neurological disorders and neurodegeneration. Indeed, polymorphisms in *GSK3B* have been implicated in Parkinson disease and *GSK3B* overexpression may be relevant to the pathogenesis of Alzheimer's disease [30]. GSK3β seems to be an essential player since lithium, which is widely used to treat mood disorders, activates the canonical pathway through GSK3β inhibition, hence inducing neurogenesis as well as improving behavior [30]. This possible link between MDD, neurodegenerative and neurological disorders, and GSK3β is an interesting avenue that deserves attention for future investigations, notably in older animals.

Funding Institutional grants were received from the Region of Lorraine (France).

Compliance with Ethical Standards

Conflict of Interest The authors declare that they have no conflict of interest.

Data Access The data discussed in this publication have been deposited in NCBI's Gene Expression Omnibus and are accessible through GEO Series accession number GSE104164 (https://www-ncbi-nlm-nih-gov.gate2.inist.fr/geo/query/acc.cgi?acc=GSE104164).

References

1. Berrocal-Zaragoza MI, Sequeira JM, Murphy MM, Fernandez-Ballart JD, Abdel Baki SG, Bergold PJ, Quadros EV (2014) Folate deficiency in rat pups during weaning causes learning and memory deficits. Br J Nutr 112:1323–1332. https://doi.org/10.1017/S0007114514002116
2. Guéant J-L, Namour F, Guéant-Rodriguez R-M, Daval J-L (2013) Folate and fetal programming: a play in epigenomics? Trends Endocrinol Metab 24:279–289. https://doi.org/10.1016/j.tem.2013.01.010
3. Smith AD, Refsum H (2016) Homocysteine, B vitamins, and cognitive impairment. Annu Rev Nutr 36:211–239. https://doi.org/10.1146/annurev-nutr-071715-050947
4. Mattson MP, Shea TB (2003) Folate and homocysteine metabolism in neural plasticity and neurodegenerative disorders. Trends Neurosci 26:137–146. https://doi.org/10.1016/S0166-2236(03)00032-8
5. Guéant J-L, Elakoum R, Ziegler O, Coelho D, Feigerlova E, Daval JL, Guéant-Rodriguez RM (2014) Nutritional models of foetal programming and nutrigenomic and epigenomic dysregulations of fatty acid metabolism in the liver and heart. Pflugers Arch 466:833–850. https://doi.org/10.1007/s00424-013-1339-4
6. Blaise SA, Nédélec E, Schroeder H, Alberto JM, Bossenmeyer-Pourié C, Guéant JL, Daval JL (2007) Gestational vitamin B deficiency leads to homocysteine-associated brain apoptosis and alters neurobehavioral development in rats. Am J Pathol 170:667–679. https://doi.org/10.2353/ajpath.2007.060339
7. El Hajj Chehadeh S, Pourié G, Martin N et al (2014) Gestational methyl donor deficiency alters key proteins involved in neurosteroidogenesis in the olfactory bulbs of newborn female rats and is associated with impaired olfactory performance. Br J Nutr 111:1021–1031. https://doi.org/10.1017/S0007114513003553
8. Kerek R, Geoffroy A, Bison A, Martin N, Akchiche N, Pourié G, Helle D, Guéant JL et al (2013) Early methyl donor deficiency may induce persistent brain defects by reducing Stat3 signaling targeted by miR-124. Cell Death Dis 4:e755. https://doi.org/10.1038/cddis.2013.278
9. Pourié G, Martin N, Bossenmeyer-Pourié C, Akchiche N, Guéant-Rodriguez RM, Geoffroy A, Jeannesson E, Chehadeh SEH et al (2015) Folate- and vitamin B12-deficient diet during gestation and lactation alters cerebellar synapsin expression via impaired influence of estrogen nuclear receptor α. FASEB J Off Publ Fed Am Soc Exp Biol 29:3713–3725. https://doi.org/10.1096/fj.14-264267
10. Bugalho P, Correa B, Viana-Baptista M (2006) Role of the cerebellum in cognitive and behavioural control: scientific basis and investigation models. Acta Medica Port 19:257–267
11. Schmahmann JD, Weilburg JB, Sherman JC (2007) The neuropsychiatry of the cerebellum—insights from the clinic. Cerebellum Lond Engl 6:254–267. https://doi.org/10.1080/14734220701490995
12. El Hajj Chehadeh S, Dreumont N, Willekens J et al (2014) Early methyl donor deficiency alters cAMP signaling pathway and neurosteroidogenesis in the cerebellum of female rat pups. Am J Physiol Endocrinol Metab 307:E1009–E1019. https://doi.org/10.1152/ajpendo.00364.2014
13. Sillitoe RV, Joyner AL (2007) Morphology, molecular codes, and circuitry produce the three-dimensional complexity of the cerebellum. Annu Rev Cell Dev Biol 23:549–577. https://doi.org/10.1146/annurev.cellbio.23.090506.123237
14. Ranade SC, Sarfaraz Nawaz M, Kumar Rambtla P, Rose AJ, Gressens P, Mani S (2012) Early protein malnutrition disrupts cerebellar development and impairs motor coordination. Br J Nutr 107:1167–1175. https://doi.org/10.1017/S0007114511004119
15. Lucas FR, Salinas PC (1997) WNT-7a induces axonal remodeling and increases synapsin I levels in cerebellar neurons. Dev Biol 192:31–44. https://doi.org/10.1006/dbio.1997.8734
16. Salinas PC, Fletcher C, Copeland NG et al (1994) Maintenance of Wnt-3 expression in Purkinje cells of the mouse cerebellum depends on interactions with granule cells. Dev Camb Engl 120:1277–1286
17. Battaglia-Hsu S, Akchiche N, Noel N, Alberto JM, Jeannesson E, Orozco-Barrios CE, Martinez-Fong D, Daval JL et al (2009) Vitamin B12 deficiency reduces proliferation and promotes differentiation of neuroblastoma cells and up-regulates PP2A, proNGF, and TACE. Proc Natl Acad Sci U S A 106:21930–21935. https://doi.org/10.1073/pnas.0811794106
18. Brazma A, Hingamp P, Quackenbush J, Sherlock G, Spellman P, Stoeckert C, Aach J, Ansorge W et al (2001) Minimum information about a microarray experiment (MIAME)-toward standards for microarray data. Nat Genet 29:365–371. https://doi.org/10.1038/ng1201-365
19. Yates A, Akanni W, Amode MR, Barrell D, Billis K, Carvalho-Silva D, Cummins C, Clapham P et al (2016) Ensembl 2016. Nucleic Acids Res 44:D710–D716. https://doi.org/10.1093/nar/gkv1157

20. Yang YH, Dudoit S, Luu P et al (2002) Normalization for cDNA microarray data: a robust composite method addressing single and multiple slide systematic variation. Nucleic Acids Res 30:e15
21. de Hoon MJL, Imoto S, Nolan J, Miyano S (2004) Open source clustering software. Bioinforma Oxf Engl 20:1453–1454. https://doi.org/10.1093/bioinformatics/bth078
22. Zeeberg BR, Feng W, Wang G, Wang MD, Fojo AT, Sunshine M, Narasimhan S, Kane DW et al (2003) GoMiner: a resource for biological interpretation of genomic and proteomic data. Genome Biol 4:R28
23. Salinas PC, Zou Y (2008) Wnt signaling in neural circuit assembly. Annu Rev Neurosci 31:339–358. https://doi.org/10.1146/annurev.neuro.31.060407.125649
24. Wisniewska MB, Nagalski A, Dabrowski M, Misztal K, Kuznicki J (2012) Novel β-catenin target genes identified in thalamic neurons encode modulators of neuronal excitability. BMC Genomics 13:635. https://doi.org/10.1186/1471-2164-13-635
25. Lucas FR, Goold RG, Gordon-Weeks PR, Salinas PC (1998) Inhibition of GSK-3beta leading to the loss of phosphorylated MAP-1B is an early event in axonal remodelling induced by WNT-7a or lithium. J Cell Sci 111(Pt 10):1351–1361
26. Inestrosa NC, Arenas E (2010) Emerging roles of Wnts in the adult nervous system. Nat Rev Neurosci 11:77–86. https://doi.org/10.1038/nrn2755
27. Shiomi K, Uchida H, Keino-Masu K, Masu M (2003) Ccd1, a novel protein with a DIX domain, is a positive regulator in the Wnt signaling during zebrafish neural patterning. Curr Biol CB 13:73–77
28. Ikeuchi Y, Stegmüller J, Netherton S et al (2009) A SnoN-Ccd1 pathway promotes axonal morphogenesis in the mammalian brain. J Neurosci 29:4312–4321. https://doi.org/10.1523/JNEUROSCI.0126-09.2009
29. Goldowitz D, Hamre K (1998) The cells and molecules that make a cerebellum. Trends Neurosci 21:375–382
30. Oliva CA, Vargas JY, Inestrosa NC (2013) Wnts in adult brain: from synaptic plasticity to cognitive deficiencies. Front Cell Neurosci 7:224. https://doi.org/10.3389/fncel.2013.00224
31. Ciani L, Krylova O, Smalley MJ, Dale TC, Salinas PC (2004) A divergent canonical WNT-signaling pathway regulates microtubule dynamics: dishevelled signals locally to stabilize microtubules. J Cell Biol 164:243–253. https://doi.org/10.1083/jcb.200309096
32. Hall AC, Lucas FR, Salinas PC (2000) Axonal remodeling and synaptic differentiation in the cerebellum is regulated by WNT-7a signaling. Cell 100:525–535
33. Ahmad-Annuar A, Ciani L, Simeonidis I, Herreros J, Fredj NB, Rosso SB, Hall A, Brickley S et al (2006) Signaling across the synapse: a role for Wnt and dishevelled in presynaptic assembly and neurotransmitter release. J Cell Biol 174:127–139. https://doi.org/10.1083/jcb.200511054
34. Ciani L, Boyle KA, Dickins E, Sahores M, Anane D, Lopes DM, Gibb AJ, Salinas PC (2011) Wnt7a signaling promotes dendritic spine growth and synaptic strength through Ca^{2+}/calmodulin-dependent protein kinase II. Proc Natl Acad Sci U S A 108:10732–10737. https://doi.org/10.1073/pnas.1018132108
35. Mentch SJ, Locasale JW (2016) One-carbon metabolism and epigenetics: understanding the specificity. Ann N Y Acad Sci 1363:91–98. https://doi.org/10.1111/nyas.12956
36. Barua S, Kuizon S, Brown WT, Junaid MA (2016) DNA methylation profiling at single-base resolution reveals gestational folic acid supplementation influences the epigenome of mouse offspring cerebellum. Front Neurosci 10:168. https://doi.org/10.3389/fnins.2016.00168
37. Pellanda H, Forges T, Bressenot A, Chango A, Bronowicki JP, Guéant JL, Namour F (2012) Fumonisin FB1 treatment acts synergistically with methyl donor deficiency during rat pregnancy to produce alterations of H3- and H4-histone methylation patterns in fetuses. Mol Nutr Food Res 56:976–985. https://doi.org/10.1002/mnfr.201100640
38. Geoffroy A, Kerek R, Pourié G, Helle D, Guéant JL, Daval JL, Bossenmeyer-Pourié C (2016) Late maternal folate supplementation rescues from methyl donor deficiency-associated brain defects by restoring Let-7 and miR-34 pathways. Mol Neurobiol 54:5017–5033. https://doi.org/10.1007/s12035-016-0035-8
39. Chen G, Broséus J, Hergalant S, Donnart A, Chevalier C, Bolaños-Jiménez F, Guéant JL, Houlgatte R (2015) Identification of master genes involved in liver key functions through transcriptomics and epigenomics of methyl donor deficiency in rat: relevance to nonalcoholic liver disease. Mol Nutr Food Res 59:293–302. https://doi.org/10.1002/mnfr.201400483